Spiro-β-lactam BSS-730A Displays Potent Activity against HIV and Plasmodium

Inês Bártolo, Bruna S. Santos, Diana Fontinha, Marta Machado, Denise Francisco, Bruno Sepodes, João Rocha, Hélder Mota-Filipe, Rui Pinto, Maria E. Figueira, Helena Barroso, Teresa Nascimento, António P. Alves de Matos, Américo J. S. Alves, Nuno G. Alves, Carlos J. V. Simões, Miguel Prudêncio, Teresa M. V. D. Pinho e Melo,* and Nuno Taveira*

Read Online

ACCESS | Metrics & More | Article Recommendations | Supporting Information

ABSTRACT: The high burden of malaria and HIV/AIDS prevents economic and social progress in developing countries. A continuing need exists for development of novel drugs and treatment regimens for both diseases in order to address the tolerability and long-term safety concerns associated with current treatment options and the emergence of drug resistance. We describe new spiro-β-lactam derivatives with potent (nM) activity against HIV and Plasmodium and no activity against bacteria and yeast. The best performing molecule of the series, BSS-730A, inhibited both HIV-1 and HIV-2 replication with an IC_{50} of 13 ± 9.59 nM and P. berghei hepatic infection with an IC_{50} of 0.55 ± 0.14 μM with a clear impact on parasite development. BSS-730A was also active against the erythrocytic stages of P. falciparum, with an estimated IC_{50} of 0.43 ± 0.04 μM. Time-of-addition studies showed that BSS-730A potentially affects all stages of the HIV replicative cycle, suggesting a complex mechanism of action. BSS-730A was active against multidrug-resistant HIV isolates, with a median 2.4-fold higher IC_{50} relative to control isolates. BSS-730A was equally active against R5 and X4 HIV isolates and displayed strong synergism with the entry inhibitor AMD3100. BSS-730A is a promising candidate for development as a potential therapeutic and/or prophylactic agent against HIV and Plasmodium.

KEYWORDS: AIDS, malaria, spiro-β-lactams, BSS-730A, anti-HIV activity, antiplasmodial activity
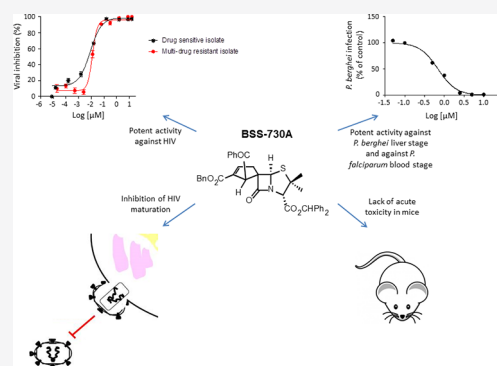
According to the most recent UNAIDS survey, at the end of 2018 almost 38 million people were living with HIV-1 and HIV-2, which continues to be the underlying cause of death for almost 1 million people every year, mostly in sub-Saharan Africa.[1] Of the four HIV-1 groups, group M is the leading cause of the AIDS pandemic, while group O has been estimated to have infected a total of around 100 000 individuals, mostly in West Central Africa, where the N and P groups have also caused sporadic cases.[2] HIV-2 is endemic in West Africa (e.g., Cape Verde, Senegal, Ivory Coast, and Guinea Bissau) and Europe (e.g., Portugal, Spain, and France).[3] An estimated 1−2 million people have been infected with HIV-2 worldwide, including those dually infected with HIV-1 and HIV-2.

As of the end of June 2019, 24.5 million people (64.6%) living with HIV were receiving antiretroviral therapy (ART), which is well short from the UNAIDS target of 81% ART coverage by 2020 and 90% coverage by 2030.[1,4] Optimal antiretroviral treatment of HIV-infected patients leads to suppression of viral replication, which prevents transmission and increases the number of CD4+ T lymphocytes thereby preventing disease progression to AIDS and death.[5] However, current drug regimens do not fully restore the health of HIV-

infected individuals[6] and rapidly select for drug-resistant strains.[7] In fact, HIV drug resistance is rising globally to levels that threat epidemic control. In 2018, only 53% (43−63%) of HIV infected people undergoing treatment were virally suppressed.[8] The prevalence of acquired drug resistance among people receiving ART ranged from 3% to 29%.[9] Among populations receiving non-nucleoside reverse transcriptase inhibitors (NNRTI)-based ART with unsuppressed viral load, the levels of NNRTI and nucleoside reverse transcriptase inhibitors (NRTI) resistance ranged from 50% to 97% and from 21% to 91%, respectively. Estimates of dual class resistance (NNRTI and NRTI) ranged between 21% and 91% of individuals for whom NNRTI-based first-line ART failed. Finally, levels of pretreatment resistance to efavirenz or nevirapine, the most widely used NNRTI drugs in first-line
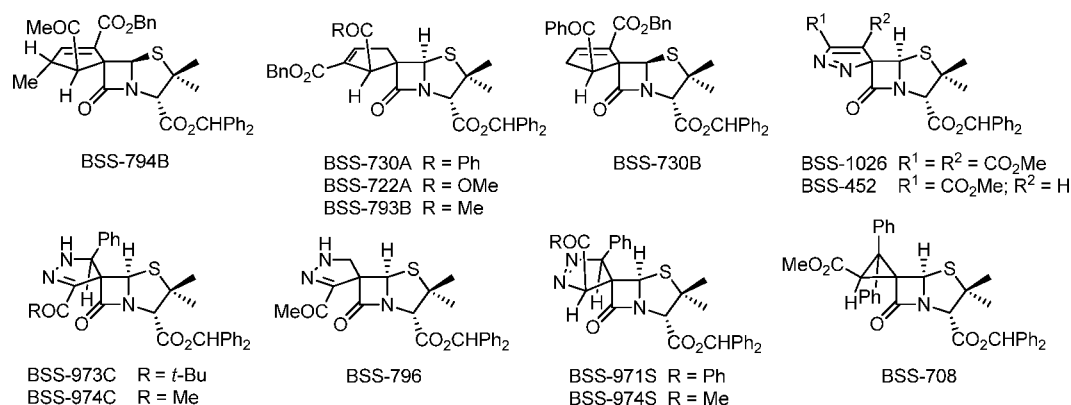
Figure 1. Structures of benzhydryl ester containing spiro-β-lactams biologically evaluated in this study.

antiretroviral treatment, exceeded 10% among adults in 12 of 18 countries that reported pretreatment drug resistance survey data to the WHO.[9] An additional challenge is that HIV-2 isolates are naturally resistant to NNRTIs and fusion inhibitors (FIs) and present a decreased sensitivity to most protease inhibitors (PIs).[10] Similarly, HIV-1 group O isolates are naturally resistant to NNRTIs and show decreased sensitivity to some protease and integrase inhibitors.[11] Hence, options available to treat patients infected with these viruses are currently very limited. Thus, a continuing need exists for development of novel drugs and regimens in order to address the tolerability and long-term safety concerns associated with current treatment options, and the emergence of drug resistance.

Malaria is caused by protozoan parasites of the *Plasmodium* genus, five species of which, *P. falciparum*, *P. ovale*, *P. vivax*, *P. malariae*, and *P. knowlesi*, are able to cause disease in humans. Malaria remains a formidable public health problem, which primarily affects the poorest regions of the world, killing nearly half a million people annually, with over 3 billion people at constant risk of infection.[12] It was estimated that in 2018 there were 228 million cases of malaria, resulting in 405 000 deaths, most of which in sub-Saharan Africa.[12] Additional tools for malaria control are urgently required, and recent calls have been made for developing new or repurposing existing drugs as valuable interventions to help control infection.[13]

The complex life cycle of *Plasmodium* parasites includes both an invertebrate host, where sexual replication occurs, and a mammalian host, where the parasite develops asexually. In the latter, the parasite undergoes a phase of replication in the liver that obligatorily precedes the blood phase of infection, responsible for disease symptoms. The asymptomatic but obligatory nature of the hepatic stage of *Plasmodium* infection makes it a privileged target for anti-plasmodial intervention, as drugs capable of inhibiting the parasite's liver stages (LS) could effectively impair infection before the onset of disease.[14−16] Moreover, *P. vivax* and *P. ovale* can produce chronic liver forms termed hypnozoites, which can remain dormant for extended periods of time before initiating a blood stage infection and causing disease relapses.[17] However, the only licensed drugs for the elimination of the hepatic forms of the parasite, primaquine and tafenaquine, have significant and potentially lethal side effects in patients with glucose-6-phosphate dehydrogenase enzyme deficiency, a common genetic trait in malaria-endemic regions. Moreover, primaquine cannot be administered to pregnant women because of its toxic effects on the fetus.[18] Because of all these limitations, it is urgent to

identify new drugs capable of eliminating the malaria parasite during the liver stage of its life cycle. Such drugs would serve not only as effective prophylactics against malaria but also as curative agents of infections caused by *P. vivax* and *P. ovale*.[18,19]

There is considerable geographic overlap between *Plasmodium* and HIV. This is particularly the case in sub-Saharan Africa, due to the presence of factors that favor transmission of either pathogen, including poverty.[20] Thus, coinfection with *Plasmodium* and HIV is common in that region and contributes to the spread and pathogenesis of both diseases.[21,22] HIV infection has been shown to increase the risk of development of severe *P. falciparum* malaria,[23−27] while malaria has been associated with a declining number of CD4+ T cells,[27] and increasing HIV-1 replication[28] and transmission levels.[21]

The β-lactam ring is the core structure of important antibiotics, such as penicillins and cephalosporins, and some monocyclic β-lactams exhibit the capacity to inhibit the HIV-1 protease.[29] Spirocyclic pyrrolidone derivatives also inhibit the HIV-1 protease.[30] More recently, it was found that some spiro-β-lactams and spiro-γ-lactams derivatives inhibit rhinovirus, poliovirus, and cytomegalovirus enzymes[31−33] and have antimalarial[34,35] activity. Given these reports, we hypothesized that new spiro-β-lactam derivatives could be developed as potent inhibitors of HIV and *Plasmodium*. In the current work, we evaluate the activity of the newly developed spiro-β-lactams against HIV, and against *P. berghei* hepatic infection and *P. falciparum* erythrocyte infection.

RESULTS

Chemistry. The synthesis of chiral spiro-β-lactams derived from 6-aminopenicillanic acid has been explored by our research group as an approach to the discovery of novel biologically active molecules.[35−39] The strategy has been to explore the reactivity of 6-diazopenicillanates and 6-alkylidenepenicillanates toward dipolarophiles and dipoles, respectively, in order to build molecules where the penicillanate core is kept and an additional medicinal chemistry structural motif is added, a spirocyclic ring system. In fact, the construction of spirocyclic frameworks is used in drug design as a way to rigidify a molecule by the fusion of two rings in one sp^3 carbon, providing a good balance of conformational rigidity and flexibility for efficient interaction with a given molecular target.[40−42] Spiro-β-lactam benzhydryl esters evaluated in this study were synthesized through previously reported synthetic

methodologies (Figure 1).[37] Studies on the deprotection of spiro-β-lactams carboxylate group to afford the corresponding more hydrophilic penicillanic acid derivatives were carried out. Deprotection of benzhydryl esters of penicillanates can be achieved by treatment with anisole, phenol, or *m*-cresol in the presence of trifluoroacetic acid.[43,44] Thus, a solution of spiro-β-lactam BSS-452 in *m*-cresol was heated at 50 °C for 3 h (Method A). However, under these reaction conditions, spiro-β-lactam BSS-452 afforded spiro-3*H*-pyrazole-β-lactam BSS-593 in only 26% yield. This yield was increased to 64% by carrying out the reaction with *m*-cresol in the presence of trifluoroacetic acid (TFA) (10 equiv) at 0 °C for 16 h (Method B). When applied to benzhydryl ester BSS-1026, these reaction conditions produced spiro-β-lactam BSS-587 with 34% yield, showing that deprotection of spiro-β-lactams requires TFA catalysis. Finally, the deprotection of the benzhydryl esters BSS-452 and BSS-1026 with anisole and TFA (25 equiv) at 5 °C for 4 h (Method C) proved to be the most efficient methodology, affording high yields of the free acids BSS-593 and BSS-587 (96 and 97%, respectively) (Figure 2).
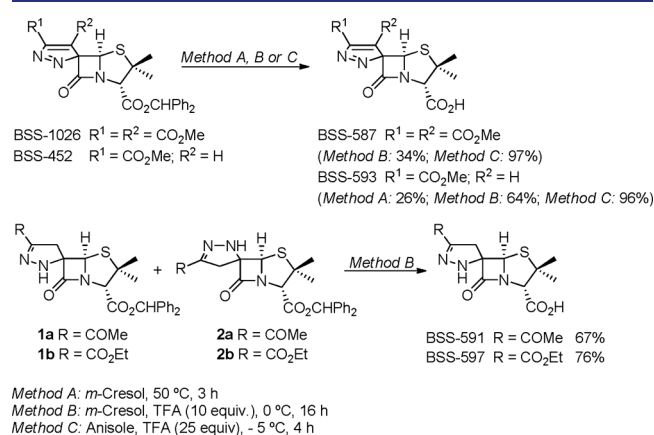

BSS-1026 $R^1 = R^2 = CO_2Me$
BSS-452 $R^1 = CO_2Me; R^2 = H$

BSS-587 $R^1 = R^2 = CO_2Me$
(*Method B*: 34%; *Method C*: 97%)
BSS-593 $R^1 = CO_2Me; R^2 = H$
(*Method A*: 26%; *Method B*: 64%; *Method C*: 96%)

1a R = COMe
1b R = CO₂Et

2a R = COMe
2b R = CO₂Et

BSS-591 R = COMe   67%
BSS-597 R = CO₂Et   76%

Method A: m-Cresol, 50 °C, 3 h
Method B: m-Cresol, TFA (10 equiv.), 0 °C, 16 h
Method C: Anisole, TFA (25 equiv), - 5 °C, 4 h

Figure 2. Deprotection of the carboxylate group of spiro-β-lactams.

Surprisingly, attempts to convert the benzhydryl esters **1** and **2** into the free acids using Method C were unsuccessful, resulting only in decomposing products. This different reaction outcome must be a result of the lower stability of the pyrazoline ring fused to the penicillanate core in these spiro-β-lactams, in comparison to the pyrazole ring present in

spirocyclic compounds BSS-1026 and BSS-452. However, the reaction of spiro-β-lactams **1** and **2** using Method B was successful, leading to the target free acids in good yield (Figure 2). These results indicate that spiro-β-lactams BSS-591 and BSS-597 are more acid-labile than spiro-β-lactams BSS-593 and BSS-587. Thus, the optimized reaction conditions for deprotection of benzhydryl esters of penicillantes are strongly dependent on the type of β-lactam derivative. It is worth emphasizing that the deprotection of spiro-β-lactams **1/2** was carried out starting from a mixture of isomers, but spiro-β-lactams BSS-591 and BSS-597 were isolated as single products after workup.

Spiro-β-lactams Cytotoxicity and Anti-HIV Activity. No significant cytotoxicity was observed *in vitro* either in TZM-bl cells or in peripheral blood mononuclear cells (PBMCs) for up to 200 μM of all spiro-β-lactams (Supplemental Table 1). The activity of spiro-β-lactams (n = 17) was evaluated in TZM-bl cells in a single-round infectivity assays against multiple HIV-1 and HIV-2 isolates, and resulted in the identification of three molecules with antiviral activity, BSS-593, BSS-722A, and BSS-730A (Table 1). BSS-593 did not inhibit HIV-2 and was a poor inhibitor of the primary HIV-1 isolate 01PTHDECJN [maximum percentage of inhibition (MPI) = 58%] (Figure 3A). In contrast, BSS-722A and BSS-730A exhibited potent activity against all HIV-1 and HIV-2 isolates (Figure 3B,C). In TZM-bl cells, the MPIs of BSS-722A and BSS-730A for both types of virus ranged from 90% to 99% (Table 1). In peripheral blood mononuclear cells (PBMCs), BSS-730A inhibited HIV-1 replication at an IC$_{50}$ of 0.075 μM, which was 5.1-fold higher than that observed in TZM-bl cells (mean IC$_{50}$ = 0.0147 μM) (Figure 3C).

BSS-730A Is Active against Multidrug Resistant HIV Isolates. The activity of BSS-730A was evaluated against eight drug-resistant HIV-2 primary isolates and the control 03PTHCC19 isolate, which is sensitive to all antiretroviral drugs in use (Table 2). BSS-730A was highly active against all but one isolate, with a median IC$_{50}$ fold-change of 2.39 and median IC$_{90}$ fold-change of 1.09 relative to the control isolate (Table 2). Isolate 03PTHDECT presented a 3.75-fold IC$_{50}$ increase in susceptibility relative to wild type, which is considered low level resistance. These results suggest that BSS-730A could be useful to treat infections caused by multidrug resistant HIV isolates.

Mechanism of Action Studies for HIV. Time-of-addition experiments were carried out to investigate which step of the HIV replicative cycle was inhibited by BSS-730A. These

Table 1. Activity of Spiro-β-lactams against HIV-1 and HIV-2 Isolates[a]

molecules	cytotoxic concentration 50% in TZM-bl cells (μM)	viruses	strain[b]	IC$_{50}$ (μM)	IC$_{90}$ (μM)	therapeutic index (CC$_{50}$/IC$_{50}$)	MPI (%)
BSS-593	158.00	HIV-1	SG3.1	0.012		13144.76	84
		HIV-1	93AOHDC249	0.035		4553.31	58
		HIV-2	03PTHCC19				
BSS-722A	53.70	HIV-1	SG3.1	0.650	1.091	82.64	97
		HIV-1	93AOHDC249	0.332	0.701	161.80	99
		HIV-2	03PTHCC19	0.510	1.182	105.29	90
BSS-730A	76.84	HIV-1	SG3.1	0.014	0.025	5584.30	99
		HIV-1	93AOHDC249	0.026	0.118	2946.32	99
		HIV-1	93AOHDC250	0.004	0.020	20247.69	94
		HIV-2	03PTHCC19	0.008	0.064	9605.00	99

[a]IC$_{50}$ - inhibitory concentration 50%; IC$_{90}$ - inhibitory concentration 90%; MPI - maximum percentage of inhibition. [b]01PTHDECJN, 93AOHDC249, 93AOHDC250, and 03PTHCC19 - primary isolates, CCR5 tropic; SG3.1 - T cell adapted isolate, CXCR4 tropic.
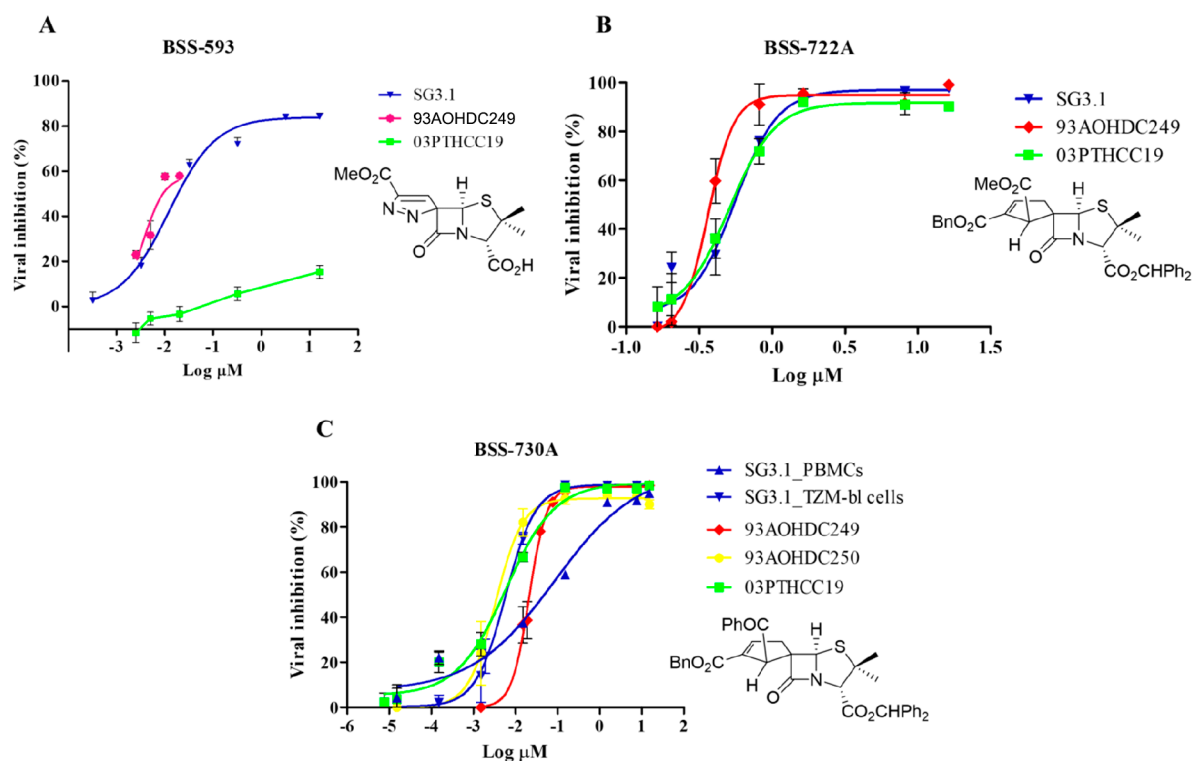
Figure 3. Activity of the different BSS molecules against HIV isolates. Dose−response curves in single cycle assay in TZM-bl cells are shown for (A) BSS-593, (B) BSS-722A, and (C) BSS-730A. SG3.1 is the reference lab adapted HIV-1 strain; 93AOHDC249 and 93AOHDC250 are primary isolates of HIV-1; 03PTHCC19 is a primary isolate of HIV-2. Inhibitory activity of BSS-730A against HIV-1 strain SG3.1 in peripheral blood mononuclear cells (PBMCs) is shown in panel C. The chemical structure of the molecules is shown in the blue inset.

Table 2. Activity of BSS-730A against Drug-Resistant Primary Isolates of HIV[a]

virus	tropism	susceptibility to antiretroviral drugs	IC$_{50}$ (μM)	IC$_{90}$ (μM)	IC$_{50}$ fold change[b]	IC$_{90}$ fold change[c]
03PTHCC19	R5	sensitive	0.008	0.064		
00PTHCC20	X4	resistant to ABC, ZDV, d4T, ddI, LPV	0.018	0.073	2.25	1.14
03PTHCC20	X4	resistant to ABC, ZDV, d4T, ddI, LPV	0.019	0.095	2.38	1.48
00PTHDECT	R5/X4	resistant to DTG	0.023	0.057	2.88	0.89
03PTHDECT	X4	resistant to DTG	0.030	0.082	3.75	1.28
03PTHSM9	X4	resistant to SQV, LPV, DRV and TAF	0.016	0.116	2.00	1.81
10PTHSJIG	R5	resistant to RAL, DTG, LPV, SQV, DRV and all NRTIs	0.012	0.032	1.50	0.50
15PTHSJIG	R5	resistant to RAL, DTG, 3TC and FTC	0.018	0.056	2.25	0.88
15PTHCEC	X4	resistant to RAL, DTG, LPV, SQV, DRV, ABC, ddI, TDF, TAF, 3TC, d4T and FTC	0.017	0.051	2.13	0.79

[a]ABC, abacavir; ZDV, zidovudine; d4T, stavudine; ddI, didanosine; 3TC, lamivudine; FTC, emtricitabine; TDF, tenofovir disoproxil fumarate; TAF, tenovovir alafenamide; LPV, lopinavir SQV, saquinavir; DRV, darunavir; DTG, dolutegravir; RAL, raltegravir; NRTIs, nucleoside reverse transcriptase inhibitors. [b]Relative to IC$_{50}$ of wild type isolate 03PTHCC19. [c]Relative to IC$_{90}$ of wild type isolate 03PTHCC19.

experiments assess how long the addition of an anti-HIV compound can be postponed within the viral replication cycle before losing its antiviral activity. For HIV-1, addition of entry inhibitors (EIs) can be delayed for 0 h, addition of reverse transcriptase inhibitors (RTIs) can be delayed for 4−5 h, addition of integrase inhibitors (IIs) can be delayed for 5−9 h, and addition of PIs can be delayed for 18−19 h after infection.[45] A significant loss of activity was not observed, even after 24 h of delay of addition of BSS-730A to the cells (Figure 4). However, BSS-730A lost 10−16% of its activity when added 15−24 h after infection, suggesting that it targets the later stages of the HIV replicative cycle, i.e., the release and/or maturation of the virus particles.

The activity of BSS-730A at several time points after the HIV-1 integration step was accessed in ACH-2 cells, a CD4-,

CD5+, transferrin receptor+, Leu-1+ T-cell clone with one integrated proviral copy of latent HIV-1 LAV.[46,47] ACH-2 cells constantly produce and secrete low levels of RT and p24 into cell culture supernatant. The cells can be induced with phorbol myristate acetate or TNF-α to secrete high levels of infectious HIV-1 but cannot be reinfected with HIV because they lack the CD4 receptor.[46,47] Similarly to darunavir, BSS-730A did not seem to inhibit the production of the virus particles in ACH-2 cells (Figure 5A), but the released particles were unable to infect and replicate in TZM-bl cells, suggesting that BSS-730A acts during the maturation phase of the virus (Figure 5B). To further address this issue, we used a single target assay to evaluate the activity of BSS-730A against one HIV-1 recombinant protease. The molecule was tested at 10 μM and showed no protease inhibitory activity (Supplemental
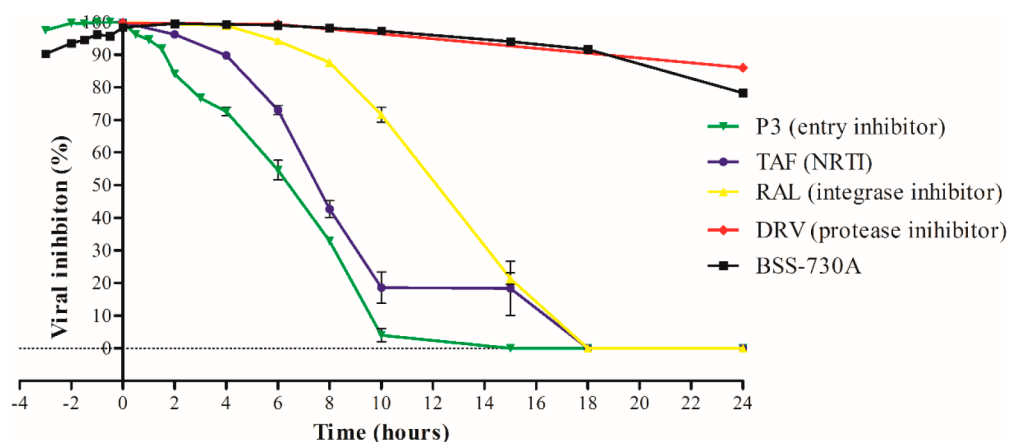
Figure 4. Time of addition assays preformed in a single-cycle inhibition assay against HIV-1 strain SG3.1. BSS-730A and control drugs targeting different steps of the HIV replication cycle were added at different time points either before or after HIV infection of TZM-bl cells. P3, peptide (fusion inhibitor); TAF, tenofovir alafanamide (nucleotide reverse transcriptase inhibitor); RAL, raltegravir (integrase inhibitor); DRV, darunavir (protease inhibitor).
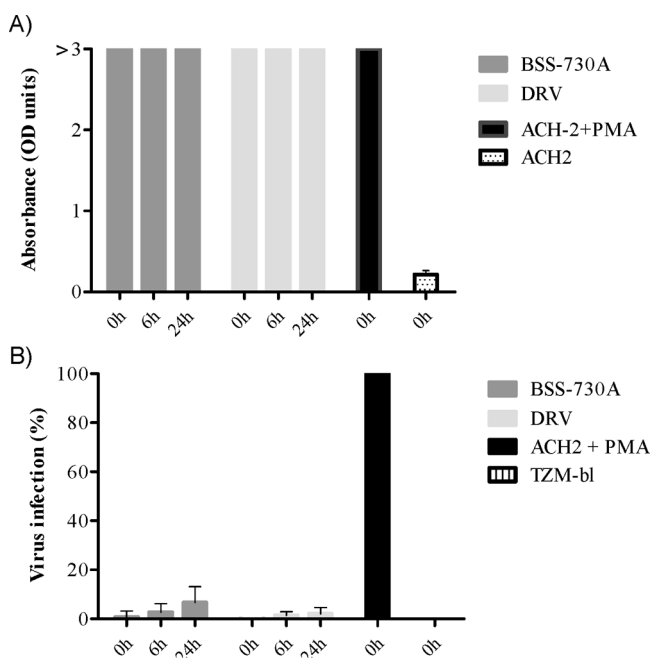

Figure 5. BSS-730A activity after the integration stage of HIV-1 as accessed in ACH-2 cells. (A) BSS-730A was added at different time points (0, 6, and 24 h) post activation of ACH2-cells with phorbol myristate. Viral p24 antigen production was determined 48 h post activation in the cell supernatant; (B) virus particles in the cell supernatant were used to infect TZM-bl cells. Infection was quantified measuring the luciferase activity after 48 h. The protease inhibitor darunavir (DRV) was used as a positive control in these experiments. The concentration of the compounds used in these experiments was two-fold the IC90 value.

Table 2). Overall, the results indicate that BSS-730A exerts its anti-HIV activity at multiple stages of the viral replicative cycle.

To explore the potential for combination with other antiretroviral drugs that target cellular components, BSS-730A was assessed in a combination with AMD3100, an entry inhibitor that binds to the CXCR4 coreceptor,[48] against HIV-1 strain SG3.1 (Supplemental Table 3). Notably, a potent synergistic activity was observed, confirming the different targets of BSS-730A and AMD3100, and suggesting that BSS-730A could be used in combination with entry inhibitors to treat or prevent HIV infection.

BSS-730A Displays Antiplasmodial Activity. The *in vitro* activity of the three spiro-β-lactams with higher anti-HIV activity, BSS-593, BSS-730A, and BSS-722A, and two non-active derivatives, BSS-452 and BSS-1026, against *P. berghei* hepatic infection was evaluated. The two molecules devoid of anti-HIV activity (BSS-452 and BSS-1026) did not display anti-*Plasmodium* activity either, whereas the ones active against HIV (BSS-593, BSS-730A, and BSS-722A) were also active against *P. berghei* liver stages (Figure 6A). Spiro-β-lactam BSS-730A was identified as the compound with the highest antiplasmodial activity, with an IC$_{50}$ of 0.55 ± 0.14 μM.

Plasmodium infection of hepatic cells comprises an initial step of invasion of the host cell and a subsequent period of intrahepatic parasite development. Thus, we sought to assess the impact of BSS-730A on either of these phases of hepatic infection *in vitro*. To this end, a GFP-expressing *P. berghei* parasite line (*Pb*GFP) was employed to infect Huh-7 cells in the presence or absence of BSS-730A, and infection was analyzed by a flow cytometry-based method.[49] Our results show that the percentage of GFP$^+$ hepatic cells is not affected by BSS-730A at its calculated IC50 (0.55 μM), indicating that BSS-730A does not affect invasion of the host cell (Figure 6B). Conversely, the addition of an equivalent amount of BSS-730A to cells after invasion by *Pb*GFP inhibited parasite development by ∼40%, as indicated by the reduction of the GFP intensity of infected cells at 48 h post infection (hpi) (Figure 6C). The dose dependency of this effect was further demonstrated (Figure 6D), confirming that it displays a clear inhibitory effect on the parasite's intrahepatic development.

Having established the *in vitro* activity of compound BSS-730A against the hepatic stage of *Plasmodium* infection, we then sought to evaluate its *in vitro* activity against the erythrocytic stages of infection by the human-infective *P. falciparum* parasite. To this end, synchronized cultures of the *P. falciparum* NF54 strain were incubated with varying amounts of BSS-730A, and the impact of this compound on parasite growth was monitored by flow cytometry following staining with a DNA dye. DMSO and chloroquine were employed as negative and positive controls in these assays, respectively. Our data show that BSS-730A effectively kills *P. falciparum* blood stages in a dose-dependent manner (Figure 7A), with an
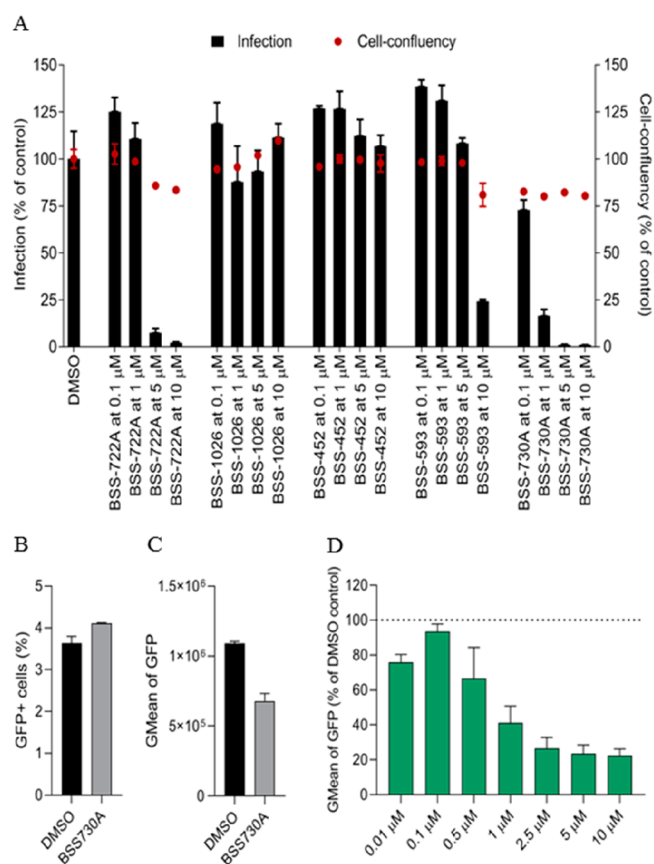
425

Figure 6. Spiro-β-lactams activity against *P. berghei* liver stages. (A) Antiplasmodial activity of four different BSS compounds (infection axis, bars) and toxicity to hepatoma cells (cell confluency axis, circles) are shown; (B, C) assessment of BSS-730A's activity against *P. berghei* invasion of hepatic cells (B) or against the intrahepatic development of *P. berghei* (C), at the compound's estimated IC50 (0.55 μM). (D) BSS-730A dose-dependence of the impairment of *P. berghei* intrahepatic development.

estimated IC$_{50}$ of 0.43 μM (Figure 7B). These results indicate that BSS-730A exerts a clear dual-stage antiplasmodial against both the hepatic and erythrocytic phases of the *Plasmodium* life cycle.

Spiro-β-lactams Lack Antibacterial and Antifungal Activity. The effect of spiro-β-lactams on common bacteria was investigated using different species of Gram-positive and Gram-negative bacteria, including two common clinical species of lactobacillus, *Lactobacillus rhamnosus* and *L. plantarum*. None of the spiro-β-lactams affected bacterial growth when employed in concentrations up to 1 mg/mL (1520 μM for BSS-730A) (Supplemental Table 4). Disk diffusion assays were employed to assess the activity of BSS-730A against three reference yeast strains: *Candida albicans* (ATCC 10231), *Candida glabrata* (ATCC 15126), and *Candida parapsilosis* (ATCC 22019). BSS-730A showed no activity against these yeast strains in concentrations up to 152 μM (Supplemental Table 5). Overall, these results show that BSS-730A displays no activity against bacteria or yeasts.

Insights from Virtual Receptor Sites via Pharmacophore Mapping Analysis. A qualitative structure–activity analysis focused on the most promising molecules showed that esterification of BSS-593 into compound BSS-452 resulted in loss of anti-HIV and anti-*Plasmodium* activity. An activity decrease was also observed in BSS-587 and its corresponding ester, BSS-1026. However, the same benzhydryl ester group is present on the highly potent molecules BSS-730A and BSS-722A. Thus, although BSS-593, BSS-722A, and BSS-730A share a spiro-β-lactamic structural core, we hypothesize that BSS-593 may bind to a site or even to a molecular target different from those to which its counterparts bind. To further explore structural similarities between these compounds, their maximum common substructure (MCS) was determined (Supplemental Figure 1). The results show that BSS-730A and BSS-722A hold a higher structural similarity with each other than with BSS-593, for which similarity is confined to the *penam* structural core that is common to all spiro-β-lactams in the series, supporting our hypothesis.

Automatically generated pharmacophore representations also support the notion that the binding site of BSS-593 differs from that of BSS-730A and BSS-722A. Even though such representations do not constitute predictive pharmaco-
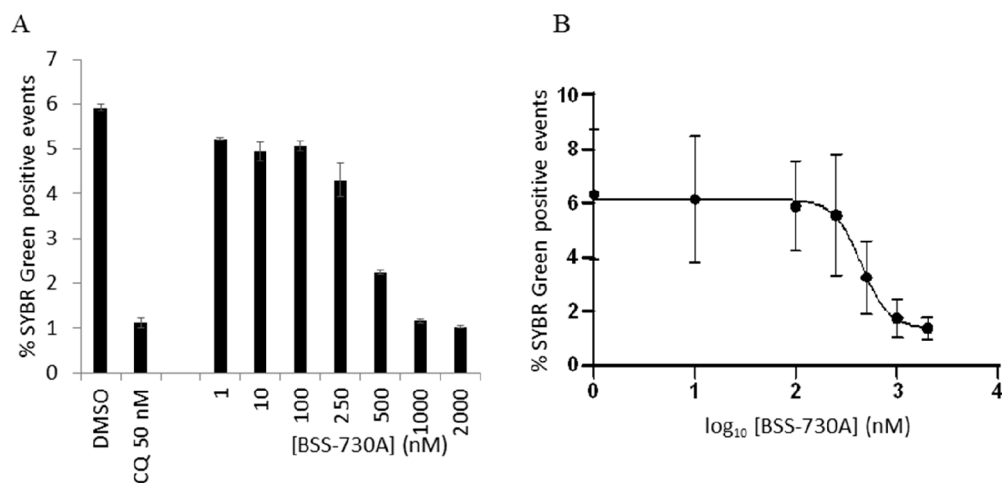

Figure 7. Inhibition of *P. falciparum* erythrocytic infection by BSS-730A. (A) Representative plot of the percentage of SYBR Green-positive events for each concentration of BSS-730A employed. DMSO and chloroquine (CQ) at 50 nM, employed as negative and positive controls, respectively, are also shown. Each data point represents the mean ± SD of triplicate measurements. (B) Dose–response curve showing the mean ± SD of three independent experiments.

phore models, given the very low number of known active compounds, we have performed pharmacophore searches in order to qualitatively assess a possible discrimination between clusters. Interestingly, representations built with the benzhydryl ester-containing active molecules as templates did not capture nonesterified spiro-β-lactams, despite their *in vitro* activity, indicating that these molecules' features cannot adjust to such a putative receptor site. Conversely, pharmacophore representations generated using spiro-β-lactams that contain a carboxylic acid on the penam's tiazolidine ring instead of on the benzhydryl ester were unable to retrieve conformers of the esterified active molecules.

In summary, these results showed that BSS-722A and BSS-730A share high similarity in terms of their structural and pharmacophoric features which differ from BSS-593. Indeed, such considerable structural and pharmacophoric differences seem to support the notion of different binding sites or targets, which could explain the superior antiviral and antiplasmodial activity of BSS-722A and BSS-730A over BSS-593.

Similarity Search. A circular extended-connectivity fingerprints (ECFP)4-based similarity search approach was used to gather insights about BSS-730A's putative mechanism of action. Such fingerprints are molecular 2D structure topological descriptors widely used for molecular characterization, similarity searching, and structure−activity modeling.[50] ECFP4 fingerprints similarity between BSS-730A and all molecules present in ChEMBL and PubChem bioactivity databases was calculated. Four molecules with anti-HIV activity were identified with a similarity coefficient (Tc) above 0.300, a reference value reported for ECFP4 fingerprints above which two molecules are likely to share the same activity.[51] These molecules, CHEMBL194164 (Tc = 0.337), CHEMBL362951 (Tc = 0.318), CHEMBL197266 (Tc = 0.310), and CHEMBL197349 (Tc = 0.306) (Supplemental Figure 2), are β-lactams and are reported as HIV protease inhibitors.[29]

Spiro-β-lactams Lack Systemic Toxicity. The acute toxicity of one member of the new spiro-β-lactams (BSS-593) was assessed in Wistar rats. Wistar rats ($n = 5$) were inoculated IP with different doses of BSS-593 (mg/kg), and effects on liver, renal, and lipid homeostasis were assessed by determining different biochemical parameters 48 h after inoculation. No significant differences between treated and untreated rats were observed, indicating that spiro-β-lactams have low systemic toxicity (Supplemental Figure 3).

■ DISCUSSION

Recent progress in the treatment and prevention of HIV/AIDS and malaria has led the United Nations to set Target 3 of its Sustainable Development Goals, which calls for ending the epidemics of HIV/AIDS and malaria by 2030.[52] Treatment and prevention of these infections rely on the use of very effective HIV-specific and *Plasmodium*-specific drugs. However, there is significant risk of interaction between antiretroviral and antimalarial drugs.[53] The mechanisms underlying such interactions may be pharmacokinetic (through enzyme inhibition or induction), pharmacodynamic (e.g., overlapping toxicities such as QT prolongation, anemia, and hepatotoxicity), or both.[53] In this setting, a drug that could work effectively against both HIV and *Plasmodium* would be ideal.

In this study, we have identified two new spiro-β-lactams derivatives with potent anti-HIV-1 and HIV-2 activity, BSS-722A and BSS-730A. BSS-730A was the best compound with a median IC$_{50}$ of 0.015 μM for HIV-1 and 0.008 μM for HIV-2. The potent activity of BSS-730A against HIV-2 is an important finding since many of the currently available antiretroviral drugs display partial or null activity against this virus.[54−56] BSS-730A was also highly active against HIV isolates that are resistant to protease inhibitors (LPV, SQV, and DRV), integrase inhibitors (RAL, DTG) and to all NRTIs. Thus, these new spiro-β-lactams or variations thereof may be particularly useful to treat or prevent infections by HIV-1, HIV-2, and drug-resistant isolates that are emerging and threatening the control of the pandemic.[9]

Remarkably, BSS-730A also displayed potent activity against *Plasmodium* hepatic stages, with a median IC$_{50}$ of 0.55 ± 0.14 μM. Additional investigations showed that the compound exerts its effect against hepatic parasites by impairing their intracellular development, following invasion of the host cells. We further showed that the compound is also active against the erythrocytic stages of *P. falciparum*, with an estimated IC$_{50}$ of 0.43 ± 0.04 μM. These results clearly show that BSS-730A exhibits multistage antiplasmodial activity, suggesting that it may act on a molecular target that is expressed throughout the parasite's life cycle. To our knowledge, this is the first spiro-β-lactam to show activity against HIV-1, HIV-2, and *Plasmodium*. Previous studies have shown that some antiretroviral drugs in clinical use, particularly protease inhibitors, exhibit some antiplasmodial activity in vitro.[57−61] Moreover, protease inhibitor-containing regimens were recently associated with reduced incidence of clinical malaria in HIV-1-infected Ugandan adults,[62] and reduced incidence of recurrent malaria in HIV-1-infected children compared with non-nucleoside reverse transcriptase inhibitor (NNRTI)-based regimens.[63]

Time-of-addition experiments showed that BSS-730A exerts its anti-HIV activity at multiple stages of the viral replicative cycle including the maturation stage of the virus although not as a formal protease inhibitor. Additional experiments are needed to identify the target and mechanism of action of BSS-730A.

CXCR4-using HIV isolates are usually found in late stages of the HIV disease and are associated with faster disease progression and drug resistance.[64−66] Currently, there is no available drug acting specifically on CXCR4-using HIV isolates. AMD3100 is a strong inhibitor of HIV-1 and HIV-2 X4 strains in vitro,[67] but its development as an antiviral was discontinued early on due to cardiac toxicity.[68] We showed that BSS-730A was very effective against X4 isolates of HIV-1 and HIV-2 and that it had a synergistic effect when combined with AMD3100. Thus, BSS-730A, either alone or in combination, might be useful to treat infections caused by CXCR4-using HIV isolates.

Structure−activity relationship analyses suggested that BSS-593 may interfere with a binding site or even a molecular target different from that of BSS-730A and BSS-722A. This suggestion stems from the identification of significant structural differences among these compounds, such as the presence of a pyrazole ring on BSS-593, instead of the cyclopentene ring present on both BSS-730A and BSS-722A, and different ring substituents on BSS-593. Consistent with their higher antiviral activity, BSS-722A and BSS-730A were shown to hold high structural similarities with each other. Thus, it may be speculated that the ring substituent groups play a major role in molecular interactions between these spiro-β-lactams and their respective targets. A similar trait has been described for other spiro compounds series.[69,70] Nevertheless, the role of the spiro-β-lactamic scaffold toward the 3D

positioning of such substituent groups should not be underestimated.[71,72]

In order to gather insights about BSS-730A's putative mechanism of action, a ECFP4 fingerprints-based similarity search using BSS-730A as a query was employed, leading to the identification of four molecules active against HIV with relevant similarity with BSS-730A (Tc > 0.3),[51] all of which were β-lactams reported as HIV protease inhibitors.[29] Besides the insights resulting from the similarity searches, an inhibitory capacity of HIV protease function would be in agreement with the time-of-addition experiments, which indicate that the molecule also acts at a late stage of HIV virus replicative cycle. Moreover, such activity could also justify BSS-730A dual activity against both HIV and *Plasmodium*, as HIV protease shows a relevant sequence and structural homology with *Plasmodium* aspartic proteases, plasmepsins,[73,74] and some commercially available HIV protease inhibitors are reported to have antiplasmodial activity.[57,75,76] However, as mentioned above, BSS-730A showed no relevant inhibitory activity against HIV protease in an enzymatic assay. Thus, the observed absence of BSS-730A HIV protease inhibitory activity, together with the time-of-addition results reported here, indicates that the molecule exerts its activity through a mechanism different from those of the currently approved anti-HIV drugs.

The target and mechanism of action of BSS-730A are still elusive. One explanation for the potent activity against two very different organisms could be that BSS-730A acts at the cell level instead of acting at the HIV or *Plasmodium* level. For example, BSS-730A may be eliciting the production of antiviral cytokines such as IFNα and/or β,[77] and antiplasmodial cytokines such as IFN-γ, which is known to control *Plasmodium* infection in both the liver and blood stages of the parasite life cycle.[78]

A potential new drug to treat or prevent virus or parasitic infections should not present antibacterial and antifungal activity, as this may promote dysbiosis of the human microflora, which is a risk factor for multiple diseases.[79,80] For example, alterations of normal vaginal microbiota may lead to bacterial vaginosis which increases the risk of vaginal HIV transmission.[81,82] We have therefore analyzed the antibacterial and antifungal activity of all our spiro-β-lactams and found that they have no effect on bacteria and fungi growth up to very high concentrations. These findings suggest that they will not affect the normal human microbiota.

In conclusion, BSS-730A potently inhibits HIV replication, including multidrug-resistant isolates, irrespective of cell tropism. BSS-730A potentially affects all stages of the HIV replicative cycle, suggesting a complex and new mechanism of action. BSS-730A further inhibits *P. falciparum* erythrocytic infection and *P. berghei* hepatic infection. BSS-730A is a promising candidate for development as a potential therapeutic and/or prophylactic agent against HIV and *Plasmodium*.

■ METHODS

Chemical Compounds. *General.* ^{1}H NMR spectra were recorded on a Bruker Avance III spectrometer operating at 400 MHz, and ^{13}C NMR spectra were recorded on the same instrument operating at 100 MHz. Tetramethylsilane (TMS) was used as an internal standard. Chemical shifts are expressed in parts per million related to TMS, and coupling constants (*J*) are in hertz. IR spectra were recorded on a Nicolet 6700 FTIR spectrometer. HRMS spectra were obtained on a VG Autospect M spectrometer (TOF MS ESI). Optical rotations

were measured on an Optical Activity AA-5 electrical polarimeter. Melting points were determined in an open glass capillary with an electrothermal melting point apparatus and are uncorrected. TLC analyses were carried out on Merck Silica gel 60 F254 plates, and flash column chromatography was performed with silica gel 60 as the stationary phase. Spiro-β-lactams BSS-794B, BSS-730A, BSS-722A, BSS-793B, BSS-730B, BSS-1026, BSS-452, BSS-973C, BSS-796, BSS-971S, BSS-974S, and BSS-708 were prepared as previously described.[37]

General Procedure for the Synthesis of Spiro-3H-pyrazole-β-lactams BSS-587, BSS-593, BSS-591, and BSS-597. Method A. A solution of the corresponding spiro-3H-pyrazole-β-lactam (0.52 mmol) in *m*-cresol (2.7 mL, 26 mmol) was stirred at 50 °C under nitrogen for 3 h. The mixture was cooled in an ice bath, and then ethyl acetate (10 mL) was added. The organic layer was extracted with saturated aqueous NaHCO$_3$ (3 × 10 mL) and then with deionized water (10 mL). The combined aqueous layers were extracted with ethyl acetate. The aqueous layer was then cooled in an ice bath to 0−5 °C and acidified to pH 1 with 10% aqueous HCl. The mixture was stirred for 30 min. The mixture was then extracted with ethyl acetate (3 × 10 mL), and the combined organic layer was dried over Na$_2$SO$_4$ and concentrated under reduced pressure.

Method B. To a mixture of the corresponding spiro-3H-pyrazole-β-lactam or spiro-2-pyrazoline-β-lactams (0.38 mmol) and *m*-cresol (0.8 mL, 7.4 mmol) at 0 °C was added TFA (0.3 mL, 3.7 mmol). The reaction mixture was stirred at 0 °C under nitrogen for 16 h. The mixture was diluted with ethyl acetate (10 mL) and was extracted with saturated aqueous NaHCO$_3$ (3 × 10 mL). The organic layer was extracted with deionized water (10 mL). The combined aqueous layers were extracted with ethyl acetate (3 × 10 mL). The aqueous layer was then cooled in an ice bath to 0−5 °C and acidified to pH 1 with 10% aqueous HCl. The mixture was stirred for 30 min. The mixture was then extracted with ethyl acetate (3 × 20 mL), and the combined organic layer was dried over Na$_2$SO$_4$ and concentrated under reduced pressure. The solid obtained was washed three times with diethyl ether/petroleum ether, and the acid was recovered by decantation.

Method C. The corresponding spiro-3H-pyrazole-β-lactam or spiro-2-pyrazoline-β-lactams (0.26 mmol) was dissolved and stirred in anhydrous CH$_2$Cl$_2$ (2 mL) at 5 °C. Anisole (0.2 mL, 1.82 mmol) and TFA (0.5 mL, 6.5 mmol) were added, and the reaction mixture was stirred for 4 h. The mixture was diluted with cold diethyl ether (10 mL), and the solvent was evaporated. The residue was dissolved in THF (5 mL) and saturated NaHCO$_3$ (15 mL) at 0 °C for 15 min and partitioned between deionized water (5 mL) and ethyl acetate (20 mL). The two layers were separated, and the aqueous layer was extracted with ethyl acetate (2 × 20 mL). The aqueous layer was acidified to pH 3 in an ice bath with HCl (1 N) and extracted with ethyl acetate (3 × 20 mL). The combined organic layer was dried over Na$_2$SO$_4$ and concentrated under reduced pressure to give the desired acid.

(2S,3′R,5R)-4′,5′-Bis(methoxycarbonyl)-3,3-dimethyl-7-oxo-4-thia-1-azaspiro[bicyclo[3.2.0]heptane-6,3′-pyrazole]-2-carboxylic acid BSS-587. Method B. Obtained from benzhydryl penicillanate BSS-1026 (205 mg, 0.38 mmol) as a yellow solid (49 mg, 0.13 mmol, 34%); Method C: Obtained from benzhydryl penicillanate BSS-1026 (167 mg, 0.31 mmol) as a yellow solid (111 mg, 0.30 mmol, 97%).

Data for compound BSS-587: mp 89−91 °C. ν_{max}/cm^{-1} (film) 3477, 1793 (β-lactam), 1744 (ester), 1589; ^{1}H NMR (400 MHz, CDCl$_3$) δ_H 1.61 (s, 3H), 1.68 (s, 3H), 3.89 (s, 3H), 4.00 (s, 3 H), 4.75 (s, 1 H), 6.02 (br s, 1H), 6.48 (s, 1 H); ^{13}C NMR (100 MHz, CDCl$_3$) δ_C 26.2, 32.1, 52.5, 53.2, 60.9, 61.4, 69.0, 110.5, 148.9, 150.0, 150.5, 160.1, 170.0, 171.0; HRMS (ESI) m/z 370.07154 (C$_{14}$H$_{16}$N$_3$O$_7$S [MH$^+$], 370.07035). $[\alpha]_{20}^D$ = +241 (c = 1.7, CH$_3$OH).

(2S,3′R,5R)-5′-(Methoxycarbonyl)-3,3-dimethyl-7-oxo-4-thia-1-azaspiro[bicyclo[3.2.0]heptane-6,3′-pyrazole]-2-carboxylic acid BSS-593. Method A. Obtained from benzhydryl penicillanate BSS-452 (253 mg, 0.53 mmol) as a yellow solid (45 mg, 0.14 mmol, 26%); Method B: Obtained from benzhydryl penicillanate BSS-452 (310 mg, 0.65 mmol) as a yellow solid (129 mg, 0.41 mmol, 64%).

Method C. Obtained from benzhydryl penicillanate BSS-452 (122 mg, 0.26 mmol) as a yellow solid (79 mg, 0.25 mmol, 96%).

Data for compound BSS-593: mp 90−91 °C. ν_{max}/cm^{-1} (film) 3469, 1783 (β-lactam), 1732 (ester), 1567; ^{1}H NMR (400 MHz, CDCl$_3$) δ_H 1.64 (s, 3H), 1.67 (s, 3H), 3.97 (s, 3H), 4.69 (s, 1 H), 4.85 (br s, 1H), 6.33 (s, 1 H), 6.87 (s, 1 H); ^{13}C NMR (100 MHz, CDCl$_3$) δ_C 26.2, 31.2, 52.7, 60.3, 61.8, 69.0, 104.4, 145.4, 149.6, 151.5, 161.8, 170.7; HRMS (ESI) m/z 312.06378 (C$_{12}$H$_{14}$N$_3$O$_5$S [MH$^+$], 312.06487). $[\alpha]_{20}^D$ = +235 (c = 1, CH$_3$OH).

Spiro[penicillanic-6,5′-(3-acetyl-2-pyrazoline)] acid BSS-591. Method B. Obtained from benzhydryl penicillanates **1a/2a** (266 mg, 0.57 mmol) as a brown solid (112 mg, 0.38 mmol, 67%).

Data for compound BSS-591: mp 152−153 °C. ν_{max}/cm^{-1} (film) 3338. 1766, 1736; ^{1}H NMR (400 MHz, CDCl$_3$) δ_H 1.54 (s, 3H), 1.57 (s, 3H), 2.41 (s, 3H), 3.23 (d, J = 18.4 Hz, 1H), 3.61 (d, J = 18.4 Hz, 1H), 4.48 (s, 1 H), 5.33 (s, 1H); ^{13}C NMR (100 MHz, CDCl$_3$) δ_C 25.6, 25.9, 33.2, 35.7, 63.6, 65.9, 68.5, 82.5, 148.2, 170.5, 173.0, 193.8; HRMS (ESI) m/z 298.08627 (C$_{12}$H$_{16}$N$_3$O$_4$S [MH$^+$], 298.08560). $[\alpha]_{20}^D$ = +145 (c = 1, CH$_3$OH).

Spiro[penicillanic-6,5′-(3-ethoxycarbonyl-2-pyrazoline)] acid BSS-597. Method B. Obtained from benzhydryl penicillanates **1b/2b** (282 mg, 0.57 mmol) as a yellow solid (142 mg, 0.43 mmol, 76%).

Data for compound BSS-597: mp 114−115 °C. ν_{max}/cm^{-1} (film) 3334, 1774, 1731, 1716; ^{1}H NMR (400 MHz, CDCl$_3$) δ_H 1.34 (t, J = 7.0 Hz, 3H), 1.54 (s, 3H), 1.56 (s, 3H), 3.30 (d, J = 18.8 Hz, 1H), 3.64 (d, J = 18.8 Hz, 1H), 4.29−4.34 (m, 2H), 4.47 (s, 1H), 5.36 (s, 1H); ^{13}C NMR (100 MHz, CDCl$_3$) δ_C 14.2, 26.0, 33.1, 37.0, 61.6, 63.6, 68.6, 77.2, 82.3, 140.0, 161.8, 170.5, 173.0; HRMS (ESI) m/z 328.09679 (C$_{13}$H$_{18}$N$_3$O$_5$S [MH$^+$], 328.09617). $[\alpha]_{20}^D$ = +140 (c = 0.5, CH$_3$OH).

Compound Clustering by the Maximum Common Substructure (MCS). The maximum common substructure (MCS) between the three spiro-β-lactams (BSS-593, 722A and 730A) and the two esterified spiro-β-lactams (BSS-722A and 730A), and between all the molecules on the presented spiro-β-lactams set was extracted using RDKit (http://www.rdkit.org) KNIME extensions within the KNIME Analytics Platform.[83]

Pharmacophore Mapping with LigandScout. The tools for automatic generation of ligand-based pharmacophores in LigandScout 4.1[84] were explored for mapping the putative pharmacophore features describing the interactions between the spiro-β-lactam compounds and their unknown target(s). Several pharmacophore representations were obtained using combinations of clustered spiro-β-lactams as a template, by considering either their merged or shared pharmacophoric features, with and without representation of exclusion volumes. A maximum of two omitted features was allowed when using the "merged features" option. Given the low number of available observations, i.e., spiro-β-lactam compounds in the series that are active against HIV and *Plasmodium*, only two active molecules were used as templates in each instance of the pharmacophore mapping procedure. Prior to alignment, all compounds had their respective conformers, i.e., their most probable three-dimensional (3D) conformations, predicted using the iCon conformer generator bundled with LigandScout, comprising the generation of a maximum of 200 conformers, with an RMSD threshold value of 0.8 to discriminate between duplicate conformations, and an energy window for conformer selection of 15 kcal/mol (standard best settings).[85] All calculated conformers were considered during the pharmacophore mapping procedure.

Similarity Search. BSS-730A 2D structure was saved in SDF format file using ChemAxon's MarvinSketch.[86] All structures from ChEMBL and PubChem bioactivity databases were downloaded also in SDF format and had smaller fragments removed to keep only the larger fragment using Open Babel software.[87] Circular Extended-Connectivity Fingerprints ECFP4[50] were used for similarity search between our query molecule, BSS-730A, and the bioactivity databases molecule sets. Calculation of both ECFP4 fingerprints and similarity coefficients, or Tanimoto, was performed using CDK software.[88]

HIV Protease Assay. BSS-730A was tested using a fluorometric assay against HIV protease to determine its inhibitory activity. The compound was tested on a concentration of 10 μM. The assay was performed as described in Toth et al.[89] The protease inhibition effect was calculated as % inhibition of protease activity; inhibition higher than 50% is considered to represent a significant effect of the test compounds.

Biological Evaluation. *Cell Lines.* TZM-bl cells (AIDS Research and Reference Reagent Program, National Institutes of Health, USA) and HEK293T cells (American Type Culture Collection) were cultured in complete growth medium that consists of Dulbecco's minimal essential medium (DMEM) supplemented with 10% fetal bovine serum (FBS), 100 U/mL of penicillin-streptomycin (Gibco/Invitrogen, USA), 1 mM of sodium pyruvate (Gibco/Invitrogen, USA), 2 mM of L-glutamine (Gibco/Invitrogen, USA), and 1 mM of nonessential amino acids (Gibco/Invitrogen, USA). Huh7 cells, a human hepatoma cell line, were cultured in RPMI medium supplemented with 10% (v/v) fetal calf serum (FCS, Gibco/Invitrogen), 1% (v/v) nonessential amino acids (Gibco/Invitrogen), 1% (v/v) glutamine (Gibco/Invitrogen), 1% (v/v) penicillin/streptomycin (pen/strep Gibco/Invitrogen), and 1% (v/v) HEPES, pH 7 (Gibco/Invitrogen) and maintained at 37 °C with 5% CO$_2$.

Peripheral blood mononuclear cells (PBMCs) from healthy individuals (blood donors) were separated by Ficoll-Paque PLUS (GE Healthcare, Waukesha, WI, USA) density gradient centrifugation and stimulated for 3 days with 5 μg/mL of phytohemaglutinin (PHA; Sigma-Aldrich, St. Louis, MO, USA). PBMCs cultures were maintained in RPMI-1640 medium supplemented with 10% FBS, 100 U/mL of

penicillin-strepotmycin, 2 mM of L-glutamine (Gibco/Invitrogen, USA), 0.3 mg/mL of gentamicin (Gibco/Invitrogen, Carlsbad, CA, USA), 5 μg/mL of Polybrene (Sigma-Aldrich, St. Louis, MO, USA), and 20 U/mL units of recombinant interleukin-2 (Roche, Basel, Switzerland). All cell cultures were maintained at 37 °C in 5% CO_2.

Cell Viability Assays. The *in vitro* cytotoxicity of spiro-β-lactams was evaluated in TZM-bl and Huh-7 cells using alamarBlue cell viability reagent (Life Technologies, USA).[90] Cells were cultured in the presence and absence of serial-fold dilutions of the spiro-β-lactam compounds. At least two independent experiments were performed for each cytotoxicity analysis. Each dilution of each compound was performed in triplicate wells. Medium controls (only growth medium), cell controls (cells without test compound), and cytotoxicity controls (a compound that kill cells) were included in each assay. The cytotoxicity of each spiro-β-lactam was expressed by the 50% cytotoxic concentration (CC_{50}), which is the concentration of compound causing a 50% decrease of cellular viability.

Antiviral Assays. The primary isolates of HIV-1 and HIV-2 used in this study were previously described and characterized for coreceptor usage and susceptibility to antiretroviral drugs.[67] The HIV-1 SG3.1 subtype B strain was obtained by transfection of HEK293T cells with pSG3.1 plasmid using jetPrime transfection reagent (Polyplus-tranfection SA, Illkirch, France) according to the manufacturer's instructions. The 50% tissue culture infectious dose ($TCID_{50}$) of each virus was determined in a single-round viral infectivity assay using a luciferase reporter gene assay in TZM-bl cells[67,91] and calculated using the statistical method of Reed and Muench.[92]

The antiviral activity of spiro-β-lactams compounds was determined in a single-round viral infectivity assay using TZM-bl reporter cells, as previously described.[67,93] Briefly, TZM-bl cells were infected with 200 $TCID_{50}$ of HIV-1 or HIV-2 in the presence of serial fold dilutions of the compounds in growth medium, supplemented with DEAE-dextran. After 48 h of infection, luciferase expression was quantified with Pierce Firefly Luc one-step glow assay kit (ThermoFisher Scientific, Rockford, USA) according to the manufacturer's instructions.

HIV inhibition assays were also done in peripheral blood mononuclear cells (PBMCs) obtained from blood donors. Phytohemaglutinin-stimulated PBMCs were infected with 200 $TCID_{50}$ of HIV-1 in the presence of serial-fold dilutions of spiro-β-lactam compounds in growth medium, followed by incubation for 7−15 days. Viral replication was measured using an antigen p24 assay (INNOTEST HIV Antigen mAb; Innogenetics, Ghent, Belgium).

At least two independent experiments were performed for each antiviral activity analysis. For each virus and compound dilution, the assay was set up in triplicate wells.

Time-of-Addition Assays. In order to investigate the mechanism of action of BSS-730A, time-of-addition assays were performed in TZM-bl cells using HIV-1 strain SG3.1 as described previously.[45,94] BSS-730A and control antiretroviral drugs (P3 peptide, a fusion inhibitor, TDF, a nucleoside RT inhibitor, RAL, a integrase inhibitor and darunavir, a protease inhibitor) were added at various time points before (−3, −2, −1.5, −1, −0.5 h) and after infection (0, 2, 4, 6, 8, 10, 15, 18, 24 h). In the former, the compound was added both to cells and viruses separately. When added to cells only, an additional washing step with PBS (twice with 200 mL) was performed before proceeding to infection. BSS-730A and control

antiretroviral drugs were added at a concentration corresponding to twice their IC_{90} value (0.1086 μM). Infection inhibition was quantified after 48 h of infection as described above.

Antiviral Assays in ACH-2 Cells. ACH-2 cells were seeded in 96-well plates (5 × 10^4 per well), activated with phorbol myristate acetate to secrete high levels of infectious HIV-1, and cultured in the presence or absence of BSS-730A at different time points after activation (0, 6, and 24 h). After 48 h, the cell supernatant was collected, and virus production was quantified using the antigen p24 assay (INNOTEST HIV Antigen mAb; Innogenetics, Ghent, Belgium). The remaining supernatant was used to infect TZM-bl cells. Infection was quantified with luciferase after 48 h. The protease inhibitor darunavir was used as a positive control in these experiments. The concentration of the compounds used in these experiments was two-fold the IC_{90} value.

Evaluation of Hepatic Stage Antiplasmodial Activity of Spiro-β-lactams. The inhibitory activity of test compounds on *in vitro* hepatic infection by *P. berghei* was determined by comparing the parasite load in compound- and solvent-treated *P. berghei*-infected Huh7 cells. Infection load was assessed by measurement of luminescence intensity in Huh-7 cells infected with a firefly luciferase-expressing *P. berghei* line, as previously described.[95,96] Briefly, Huh-7 cells were seeded in 96-well plates (1.0 × 10^4 cells per well) the day before drug treatment and infection. The medium was replaced by medium containing the appropriate concentration of each compound approximately 1 h prior to infection with sporozoites freshly obtained through disruption of salivary glands of infected female *Anopheles stephensi* mosquitoes. Sporozoite addition was followed by centrifugation at 1700g for 5 min. Parasite infection load was measured 48 h after infection by a bioluminescence assay (Biotium). Cell confluence, a surrogate measure of compound toxicity to Huh7 cells, was measured by fluorescence measurements using the AlamarBlue assay, according to the manufacturer's instructions. All compounds were initially screened at 0.1, 1, 5, and 10 μM, and the IC_{50} of compound BSS-730A was determined by evaluating the activity of the drug at seven different concentrations ranging from 0.1 to 10 μM.

The discrimination of the activity of BSS-730A against parasite invasion or intrahepatic development was assessed by flow cytometry analysis of Huh7 cells infected with a GFP-expressing *P. berghei* line (PbGFP), as previously described.[49] To assess the impact in invasion, BSS-730A was added 1 h prior to infection, and samples were collected and analyzed at 2 hpi, to determine the percentage of GFP$^+$ cells. To assess development, the compound was present from 2 up to 48 hpi, at which point samples were collected and analyzed to assess the GFP intensity of infected cells. Cells were analyzed on a BD Accuri C6 (BD Biosciences). Data acquisition and analysis were carried out using the Accuri C6 (version 1.0.264.21, BD) and FlowJo (version 10.0.8, FlowJo) software packages, respectively.

Evaluation of Blood Stage Antiplasmodial Activity of BSS-730A. Ring-stage synchronized cultures of *P. falciparum* strain NF54 at 2.5% hematocrit and at approximately 1% parasitemia were incubated with test compounds or dimethyl sulfoxide (DMSO, vehicle control) in 96-well plates, for 48 h, at 37 °C in a 5% CO_2 and 5% O_2 atmosphere. Stock solutions of chloroquine (positive control) and BSS-730A were prepared in DMSO. Working solutions were prepared from the stock solutions in complete malaria culture medium (CMCM),

which consists of RPMI 1640 supplemented with 25 mM HEPES, 2.4 mM L-glutamine, 50 μg/mL gentamicin, 0.5% w/v Albumax, 11 mM glucose, 1.47 mM hypoxanthine, and 37.3 mM NaHCO$_3$. For each measurement, 5 μL of the culture (approximately 800 000 cells) were stained with the DNA-specific dye SYBR green I. After 20 min of incubation in the dark, the stained sample was analyzed by flow cytometry. Approximately 100 000 events were analyzed in each flow cytometry measurement. Two independent experiments were performed, and all samples were analyzed in triplicate.

Ethics Statement. Experiments were conducted according to the Home Office Guidance in the Operation of Animals (Scientific Procedures) Act 1986, published by Her Majesty's Stationary Office, London, UK, and the Institutional Animal Research Committee Guide for the Care and Use of Laboratory Animals published by the U.S. National Institutes of Health (NIH Publication No. 85-23, revised 1996), as well as to the currently adopted EC regulations. Finally, the studies are in compliance with the ARRIVE Guidelines for Reporting Animal Research' summarized at www.nc3rs.org.uk. Authors B.S. and J.B. are licensed by the Portuguese General Directorate of Alimentation and Veterinary to coordinate and conduct independent animal research.

Statistical Analysis. Statistical analysis was performed using Prism version 5.01 for Windows (GrahPad Software, San Diego, California USA, www.graphpad.com) with a level of significance of 5%. The 50% (IC$_{50}$) and 90% (IC$_{90}$) inhibitory concentrations, as well as the dose−response curve slopes (Hill slope), were estimated by plotting the percent inhibition of infection (y axis) against the log10 concentration of each spiro-lactam compound (x axis) and using the sigmoidal dose−response (variable slope) equation. The F-test was used to compare best-fit values of dose−response curves of drug-resistant and drug-sensitive isolates.

The results of both the cytotoxicity and *in vivo* acute toxicity assays were expressed as the means with their standard errors and were compared using a one-factorial ANOVA test, followed by a Bonferroni's multicomparison post hoc test. A P value less than 0.05 was considered to be statistically significant.

■ ASSOCIATED CONTENT

Ⓢ Supporting Information

The Supporting Information is available free of charge at https://pubs.acs.org/doi/10.1021/acsinfecdis.0c00768.

Supplemental Table 1 - Cytotoxic concentration of spiro-β-lactams in TZM-bl cells. Supplemental Table 2 - HIV-1 protease inhibition by BSS-730A. Supplemental Table 3 - Combination indices (CI) of different AMD3100: BSS-730A combinations against HIV-1$_{SG3.1}$. Supplemental Table 4 - Antibacterial activity of spiro-β-lactams. Supplemental Table 5 - Antifungal activity of BSS-730A in agar diffusion assay. Supplemental Figure 1, Supplemental Figure 2, Supplemental Figure 3 - Acute toxicity assay of compound BSS-593. Materials and Methods (PDF)

■ AUTHOR INFORMATION

Corresponding Authors

Nuno Taveira − *Instituto de investigação do Medicamento (iMed.ULisboa), Faculdade de Farmácia, Universidade de Lisboa, 1649-003 Lisbon, Portugal; Centro de Investigação Interdisciplinar Egas Moniz (CiiEM), Instituto Universitário Egas Moniz, 2829-511 Monte da Caparica, Portugal;* ⓞ orcid.org/0000-0003-0176-5585; Email: ntaveira@ff.ulisboa.pt

Teresa M. V. D. Pinho e Melo − *Coimbra Chemistry Centre (CQC), Department of Chemistry, University of Coimbra, 3004-535 Coimbra, Portugal;* ⓞ orcid.org/0000-0003-3256-4954; Email: tmelo@ci.uc.pt

Authors

Inês Bártolo − *Instituto de investigação do Medicamento (iMed.ULisboa), Faculdade de Farmácia, Universidade de Lisboa, 1649-003 Lisbon, Portugal*

Bruna S. Santos − *Coimbra Chemistry Centre (CQC), Department of Chemistry, University of Coimbra, 3004-535 Coimbra, Portugal*

Diana Fontinha − *Instituto de Medicina Molecular João Lobo Antunes, Faculdade de Medicina, Universidade de Lisboa, 1648-028 Lisboa, Portugal*

Marta Machado − *Instituto de Medicina Molecular João Lobo Antunes, Faculdade de Medicina, Universidade de Lisboa, 1648-028 Lisboa, Portugal*

Denise Francisco − *Instituto de Medicina Molecular João Lobo Antunes, Faculdade de Medicina, Universidade de Lisboa, 1648-028 Lisboa, Portugal*

Bruno Sepodes − *Instituto de investigação do Medicamento (iMed.ULisboa), Faculdade de Farmácia, Universidade de Lisboa, 1649-003 Lisbon, Portugal*

João Rocha − *Instituto de investigação do Medicamento (iMed.ULisboa), Faculdade de Farmácia, Universidade de Lisboa, 1649-003 Lisbon, Portugal*

Hélder Mota-Filipe − *Instituto de investigação do Medicamento (iMed.ULisboa), Faculdade de Farmácia, Universidade de Lisboa, 1649-003 Lisbon, Portugal*

Rui Pinto − *Instituto de investigação do Medicamento (iMed.ULisboa), Faculdade de Farmácia, Universidade de Lisboa, 1649-003 Lisbon, Portugal*

Maria E. Figueira − *Instituto de investigação do Medicamento (iMed.ULisboa), Faculdade de Farmácia, Universidade de Lisboa, 1649-003 Lisbon, Portugal*

Helena Barroso − *Centro de Investigação Interdisciplinar Egas Moniz (CiiEM), Instituto Universitário Egas Moniz, 2829-511 Monte da Caparica, Portugal*

Teresa Nascimento − *Centro de Investigação Interdisciplinar Egas Moniz (CiiEM), Instituto Universitário Egas Moniz, 2829-511 Monte da Caparica, Portugal*

António P. Alves de Matos − *Centro de Investigação Interdisciplinar Egas Moniz (CiiEM), Instituto Universitário Egas Moniz, 2829-511 Monte da Caparica, Portugal*

Américo J. S. Alves − *Coimbra Chemistry Centre (CQC), Department of Chemistry, University of Coimbra, 3004-535 Coimbra, Portugal*

Nuno G. Alves − *Coimbra Chemistry Centre (CQC), Department of Chemistry, University of Coimbra, 3004-535 Coimbra, Portugal*

Carlos J. V. Simões − *Coimbra Chemistry Centre (CQC), Department of Chemistry, University of Coimbra, 3004-535 Coimbra, Portugal*

Miguel Prudêncio − *Instituto de Medicina Molecular João Lobo Antunes, Faculdade de Medicina, Universidade de Lisboa, 1648-028 Lisboa, Portugal*

Complete contact information is available at:
https://pubs.acs.org/10.1021/acsinfecdis.0c00768

REFERENCES

(1) *Global HIV & AIDS Statistics-2019 Fact Sheet*; UNAIDS: Geneve, 2020.

(2) Hemelaar, J., Elangovan, R., Yun, J., Dickson-Tetteh, L., Fleminger, I., Kirtley, S., Williams, B., Gouws-Williams, E., and Ghys, P. D. (2019) Global and regional molecular epidemiology of HIV-1, 1990−2015: a systematic review, global survey and trend analysis. *Lancet Infect Dis. 19* (2), 143−155.

(3) Gottlieb, G. S., Raugi, D. N., and Smith, R. A. (2018) 90−90−90 for HIV-2? Ending the HIV-2 epidemic by enhancing care and clinical management of patients infected with HIV-2. *Lancet HIV 5* (7), e390−e399.

(4) *Understanding Fast-Track; Accelerating Action to End the AIDS Epidemic by 2030*; UNAIDS: Geneva, 2015.

(5) Gunthard, H. F., Saag, M. S., Benson, C. A., del Rio, C., Eron, J. J., Gallant, J. E., Hoy, J. F., Mugavero, M. J., Sax, P. E., Thompson, M. A., Gandhi, R. T., Landovitz, R. J., Smith, D. M., Jacobsen, D. M., and Volberding, P. A. (2016) Antiretroviral Drugs for Treatment and Prevention of HIV Infection in Adults: 2016 Recommendations of the International Antiviral Society-USA Panel. *Jama 316* (2), 191−210.

(6) Solomon, D. A., and Sax, P. E. (2015) Current state and limitations of daily oral therapy for treatment. *Curr. Opin. HIV AIDS 10* (4), 219−225.

(7) Chen, T. K., and Aldrovandi, G. M. (2008) Review of HIV antiretroviral drug resistance. *Pediatr Infect Dis J. 27* (8), 749−752.

(8) *Global AIDS Update 2019*; UNAIDS: Geneva, 2019.

(9) *HIV Drug Resistance Report 2019*; World Health Organization: Geneva, 2019.

(10) Tzou, P. L., Descamps, D., Rhee, S. Y., Raugi, D. N., Charpentier, C., Taveira, N., Smith, R. A., Soriano, V., de Mendoza, C., Holmes, S. P., Gottlieb, G. S., and Shafer, R. W. (2020) Expanded Spectrum of Antiretroviral-Selected Mutations in Human Immuno-deficiency Virus Type 2. *J. Infect. Dis. 221* (12), 1962−1972.

(11) Tebit, D. M., Patel, H., Ratcliff, A., Alessandri, E., Liu, J., Carpenter, C., Plantier, J. C., and Arts, E. J. (2016) HIV-1 Group O Genotypes and Phenotypes: Relationship to Fitness and Susceptibility to Antiretroviral Drugs. *AIDS Res. Hum. Retroviruses 32* (7), 676−88.

(12) *World Malaria Report 2019*; World Health Organization: Geneva, 2019.

(13) Alonso, P. L., Brown, G., Arevalo-Herrera, M., Binka, F., Chitnis, C., Collins, F., Doumbo, O. K., Greenwood, B., Hall, B. F., Levine, M. M., Mendis, K., Newman, R. D., Plowe, C. V., Rodriguez, M. H., Sinden, R., Slutsker, L., and Tanner, M. (2011) A research agenda to underpin malaria eradication. *PLoS Med. 8* (1), e1000406.

(14) Prudencio, M., Rodriguez, A., and Mota, M. M. (2006) The silent path to thousands of merozoites: the Plasmodium liver stage. *Nat. Rev. Microbiol. 4* (11), 849−956.

(15) Rodrigues, T., Prudencio, M., Moreira, R., Mota, M. M., and Lopes, F. (2012) Targeting the liver stage of malaria parasites: a yet unmet goal. *J. Med. Chem. 55* (3), 995−1012.

(16) Derbyshire, E. R., Prudencio, M., Mota, M. M., and Clardy, J. (2012) Liver-stage malaria parasites vulnerable to diverse chemical scaffolds. *Proc. Natl. Acad. Sci. U. S. A. 109* (22), 8511−8516.

(17) White, N. J., and Imwong, M. (2012) Relapse. *Adv. Parasitol. 80*, 113−150.

(18) Vale, N., Moreira, R., and Gomes, P. (2009) Primaquine revisited six decades after its discovery. *Eur. J. Med. Chem. 44* (3), 937−953.

(19) Baird, J. K., and Hoffman, S. L. (2004) Primaquine therapy for malaria. *Clin. Infect. Dis. 39* (9), 1336−1345.

(20) Njunda, A. L., Njumkeng, C., Nsagha, S. D., Assob, J. C., and Kwenti, T. E. (2016) The prevalence of malaria in people living with HIV in Yaounde, Cameroon. *BMC Public Health 16*, 964.

(21) Abu-Raddad, L. J., Patnaik, P., and Kublin, J. G. (2006) Dual infection with HIV and malaria fuels the spread of both diseases in sub-Saharan Africa. *Science 314* (5805), 1603−1606.

(22) Skinner-Adams, T. S., McCarthy, J. S., Gardiner, D. L., and Andrews, K. T. (2008) HIV and malaria co-infection: interactions and consequences of chemotherapy. *Trends Parasitol. 24* (6), 264−271.

(23) Cohen, C., Karstaedt, A., Frean, J., Thomas, J., Govender, N., Prentice, E., Dini, L., Galpin, J., and Crewe-Brown, H. (2005) Increased prevalence of severe malaria in HIV-infected adults in South Africa. *Clin. Infect. Dis. 41* (11), 1631−1637.

(24) Flateau, C., Le Loup, G., and Pialoux, G. (2011) Consequences of HIV infection on malaria and therapeutic implications: a systematic review. *Lancet Infect. Dis. 11* (7), 541−556.

(25) Grimwade, K., French, N., Mbatha, D. D., Zungu, D. D., Dedicoat, M., and Gilks, C. F. (2004) HIV infection as a cofactor for severe falciparum malaria in adults living in a region of unstable malaria transmission in South Africa. *AIDS 18* (3), 547−554.

(26) Otieno, R. O., Ouma, C., Ong'echa, J. M., Keller, C. C., Were, T., Waindi, E. N., Michaels, M. G., Day, R. D., Vulule, J. M., and Perkins, D. J. (2006) Increased severe anemia in HIV-1-exposed and HIV-1-positive infants and children during acute malaria. *AIDS 20* (2), 275−280.

(27) Patnaik, P., Jere, C. S., Miller, W. C., Hoffman, I. F., Wirima, J., Pendame, R., Meshnick, S. R., Taylor, T. E., Molyneux, M. E., and Kublin, J. G. (2005) Effects of HIV-1 serostatus, HIV-1 RNA concentration, and CD4 cell count on the incidence of malaria infection in a cohort of adults in rural Malawi. *J. Infect. Dis. 192* (6), 984−991.

(28) Kublin, J. G., Patnaik, P., Jere, C. S., Miller, W. C., Hoffman, I. F., Chimbiya, N., Pendame, R., Taylor, T. E., and Molyneux, M. E. (2005) Effect of Plasmodium falciparum malaria on concentration of

HIV-1-RNA in the blood of adults in rural Malawi: a prospective cohort study. *Lancet* 365 (9455), 233–240.

(29) Sperka, T., Pitlik, J., Bagossi, P., and Tozser, J. (2005) Beta-lactam compounds as apparently uncompetitive inhibitors of HIV-1 protease. *Bioorg. Med. Chem. Lett.* 15 (12), 3086–3090.

(30) Kazmierski, W. M., Furfine, E., Spaltenstein, A., and Wright, L. L. (2002) Novel spirocyclic pyrrolidones as P2/P1 mimetics in potent inhibitors of HIV-1 protease. *Bioorg. Med. Chem. Lett.* 12 (23), 3431–3433.

(31) Gabriel, S. D., and Rotstein, D. M. (2008) *Heterocyclic antiviral compounds*, (U.S. Patent No. 2008139544). European Patent Office. http://europepmc.org/patents/PAT/US2008139544.

(32) Mehta, P. D., Sengar, N. P. S., and Pathak, A. K. (2010) 2-Azetidinone - A new profile of various pharmacological activities. *Eur. J. Med. Chem.* 45 (12), 5541–5560.

(33) Skiles, J. W., and McNeil, D. (1990) Spiro indolinone beta-lactams, inhibitors of poliovirus and rhinovlrus 3C-proteinases. *Tetrahedron Lett.* 31, 7277–7280.

(34) Jarrahpour, A., Ebrahimi, E., De Clercq, E., Sinou, V., Latour, C., Djouhri Bouktab, L., and Brunel, J. M. (2011) Synthesis of mono-, bis-spiro- and dispiro-β-lactams and evaluation of their antimalarial activities. *Tetrahedron* 67 (45), 8699–8704.

(35) Alves, A. J.S., Alves, N. G., Caratao, C. C., Esteves, M. I.M., Fontinha, D., Bartolo, I., Soares, M. I.L., Lopes, S. M.M., Prudencio, M., Taveira, N., and Pinho e Melo, T. M.V.D. (2020) Spiro-Lactams as Novel Antimicrobial Agents. *Curr. Top. Med. Chem.* 20 (2), 140–152.

(36) Santos, B. S., Gomes, C. S.B., and Pinho e Melo, T. M.V.D. (2014) Synthesis of chiral spiropyrazoline-beta-lactams and spirocyclopropyl-beta-lactams from 6-alkylidenepenicillanates. *Tetrahedron* 70 (24), 3812–3821.

(37) Santos, B. S., Nunes, S. C. C., Pais, A. A. C. C., and Pinho e Melo, T. M.V.D. (2012) Chiral spiro-beta-lactams from 6-diazopenicillanates. *Tetrahedron* 68 (19), 3729–3737.

(38) Alves, A. J. S., and Pinho e Melo, T. M. V. D. (2020) Synthesis of Novel Chiral Spiroisoxazolidine-β-Lactams from 6-Alkylidenepenicillanates: A 1,3-Dipolar Cycloaddition Approach. *Eur. J. Org. Chem.*, 6259–6269.

(39) Santos, B. S., and Pinho e Melo, T. M. V. D. (2013) Synthesis of Chiral Spirocyclopentenyl-beta-lactams through Phosphane-Catalyzed [3 + 2] Annulation of Allenoates with 6-Alkylidenepenicillanates. *Eur. J. Org. Chem.* 2013, 3901–3909.

(40) Chaubet, G., Coursindel, T., Morelli, X., Betzi, S., Roche, P., Guari, Y., Lebrun, A., Toupet, L., Collette, Y., Parrot, I., and Martinez, J. (2013) Stereoselective synthesis of original spirolactams displaying promising folded structures. *Org. Biomol. Chem.* 11 (28), 4719–4726.

(41) Zheng, Y., Tice, C. M., and Singh, S. B. (2014) The use of spirocyclic scaffolds in drug discovery. *Bioorg. Med. Chem. Lett.* 24 (16), 3673–3682.

(42) Chupakhin, E., Babich, O., Prosekov, A., Asyakina, L., and Krasavin, M., Spirocyclic Motifs in Natural Products. *Molecules* 2019, 24 (22), 4165.

(43) Torii, S., Tanaka, H., Taniguchi, M., Kameyama, Y., Sasaoka, M., Shiroi, T., Kikuchi, R., Kawahara, I., Shimabayashi, A., and Nagao, S. (1991) Deprotection of carboxylic esters of.beta.-lactam homologs. Cleavage of p-methoxybenzyl, diphenylmethyl, and tert-butyl esters effected by a phenolic matrix. *J. Org. Chem.* 56 (11), 3633–3637.

(44) Chen, P. C., Wharton, R. E., Patel, P. A., and Oyelere, A. K. (2007) Direct diazo-transfer reaction on β-lactam: Synthesis and preliminary biological activities of 6-triazolylpenicillanic acids. *Bioorg. Med. Chem.* 15 (23), 7288–7300.

(45) Pannecouque, C., Pluymers, W., Van Maele, B., Tetz, V., Cherepanov, P., De Clercq, E., Witvrouw, M., and Debyser, Z. (2002) New class of HIV integrase inhibitors that block viral replication in cell culture. *Curr. Biol.* 12 (14), 1169–1177.

(46) Folks, T. M., Clouse, K. A., Justement, J., Rabson, A., Duh, E., Kehrl, J. H., and Fauci, A. S. (1989) Tumor necrosis factor alpha induces expression of human immunodeficiency virus in a chronically infected T-cell clone. *Proc. Natl. Acad. Sci. U. S. A.* 86 (7), 2365–2368.

(47) Clouse, K. A., Powell, D., Washington, I., Poli, G., Strebel, K., Farrar, W., Barstad, P., Kovacs, J., Fauci, A. S., and Folks, T. M. (1989) Monokine regulation of human immunodeficiency virus-1 expression in a chronically infected human T cell clone. *J. Immunol.* 142 (2), 431–438.

(48) Hatse, S., Princen, K., Gerlach, L. O., Bridger, G., Henson, G., De Clercq, E., Schwartz, T. W., and Schols, D. (2001) Mutation of Asp(171) and Asp(262) of the chemokine receptor CXCR4 impairs its coreceptor function for human immunodeficiency virus-1 entry and abrogates the antagonistic activity of AMD3100. *Mol. Pharmacol.* 60 (1), 164–173.

(49) Prudencio, M., Rodrigues, C. D., Ataide, R., and Mota, M. M. (2007) Dissecting in vitro host cell infection by Plasmodium sporozoites using flow cytometry. *Cell. Microbiol.* 10 (1), 218–224.

(50) Rogers, D., and Hahn, M. (2010) Extended-Connectivity Fingerprints. *J. Chem. Inf. Model.* 50 (5), 742–754.

(51) Jasial, S., Hu, Y., Vogt, M., and Bajorath, J., Activity-relevant similarity values for fingerprints and implications for similarity searching. *F1000Research* 2016, 5, 591.

(52) *Goal 3: Ensure healthy lives and promote well-being for all at all ages. United Nations 410 Sustainable Development Goals.* https://www.un.org/sustainabledevelopment/health/.

(53) Seden, K., Gibbons, S., Marzolini, C., Schapiro, J. M., Burger, D. M., Back, D. J., and Khoo, S. H. (2017) Development of an evidence evaluation and synthesis system for drug-drug interactions, and its application to a systematic review of HIV and malaria co-infection. *PLoS One* 12 (3), No. e0173509.

(54) Witvrouw, M., Pannecouque, C., Switzer, W. M., Folks, T. M., De Clercq, E., and Heneine, W. (2004) Susceptibility of HIV-2, SIV and SHIV to various anti-HIV-1 compounds: implications for treatment and postexposure prophylaxis. *Antivir. Ther.* 9 (1), 57–65.

(55) Camacho, R. J. (2012) Special aspects of the treatment of HIV-2-infected patients. *Intervirology* 55 (2), 179–183.

(56) de Mendoza, C., Lozano, A. B., Caballero, E., Cabezas, T., Ramos, J. M., and Soriano, V. (2020) Antiretroviral Therapy for HIV-2 Infection in Non-Endemic Regions. *AIDS Rev.* 22 (1), 44–56.

(57) Nsanzabana, C., and Rosenthal, P. J. (2011) In vitro activity of antiretroviral drugs against Plasmodium falciparum. *Antimicrob. Agents Chemother.* 55 (11), 5073–5077.

(58) Parikh, S., Gut, J., Istvan, E., Goldberg, D. E., Havlir, D. V., and Rosenthal, P. J. (2005) Antimalarial activity of human immunodeficiency virus type 1 protease inhibitors. *Antimicrob. Agents Chemother.* 49 (7), 2983–2985.

(59) Machado, M., Sanches-Vaz, M., Cruz, J. P., Mendes, A. M., and Prudencio, M. (2017) Inhibition of Plasmodium Hepatic Infection by Antiretroviral Compounds. *Front. Cell. Infect. Microbiol.* 7, 329.

(60) Azevedo, R., Mendes, A. M., and Prudencio, M. (2020) The Impact of Antiretroviral Therapy on Malaria Parasite Transmission. *Front. Microbiol.* 10, 3048.

(61) Skinner-Adams, T. S., McCarthy, J. S., Gardiner, D. L., Hilton, P. M., and Andrews, K. T. (2004) Antiretrovirals as antimalarial agents. *J. Infect. Dis.* 190 (11), 1998–2000.

(62) Kasirye, R. P., Grosskurth, H., Munderi, P., Levin, J., Anywaine, Z., Nunn, A., Kamali, A., and Baisley, K. (2017) Effect of antiretroviral therapy on malaria incidence in HIV-infected Ugandan adults. *AIDS* 31 (4), 577–582.

(63) Achan, J., Kakuru, A., Ikilezi, G., Ruel, T., Clark, T. D., Nsanzabana, C., Charlebois, E., Aweeka, F., Dorsey, G., Rosenthal, P. J., Havlir, D., and Kamya, M. R. (2012) Antiretroviral agents and prevention of malaria in HIV-infected Ugandan children. *N. Engl. J. Med.* 367 (22), 2110–2118.

(64) Maartens, G., Celum, C., and Lewin, S. R. (2014) HIV infection: epidemiology, pathogenesis, treatment, and prevention. *Lancet* 384 (9939), 258–271.

(65) Green, T. N., Archary, M., Gordon, M. L., Padayachi, N., Lie, Y., Anton, E. D., Reeves, J. D., Grobler, A., Bobat, R., Coovadia, H., and Ndung'u, T. (2012) Drug resistance and coreceptor usage in HIV

type 1 subtype C-infected children initiating or failing highly active antiretroviral therapy in South Africa. *AIDS Res. Hum. Retroviruses* 28 (4), 324−32.

(66) Marcelino, J. M., Borrego, P., Nilsson, C., Familia, C., Barroso, H., Maltez, F., Doroana, M., Antunes, F., Quintas, A., and Taveira, N. (2012) Resistance to antibody neutralization in HIV-2 infection occurs in late stage disease and is associated with X4 tropism. *AIDS* 26 (18), 2275−2284.

(67) Borrego, P., Calado, R., Marcelino, J. M., Bartolo, I., Rocha, C., Cavaco-Silva, P., Doroana, M., Antunes, F., Maltez, F., Caixas, U., Barroso, H., and Taveira, N. (2012) Baseline susceptibility of primary HIV-2 to entry inhibitors. *Antiviral Ther.* 17 (3), 565−570.

(68) Hendrix, C. W., Collier, A. C., Lederman, M. M., Schols, D., Pollard, R. B., Brown, S., Jackson, J. B., Coombs, R. W., Glesby, M. J., Flexner, C. W., Bridger, G. J., Badel, K., MacFarland, R. T., Henson, G. W., and Calandra, G. (2004) Safety, pharmacokinetics, and antiviral activity of AMD3100, a selective CXCR4 receptor inhibitor, in HIV-1 infection. *JAIDS, J. Acquired Immune Defic. Syndr.* 37 (2), 1253−1262.

(69) Yamato, M., Hashigaki, K., Ikeda, M., Ohtake, H., and Tasaka, K. (1981) Synthesis and structure-activity relationship of spiro-[isochromanpiperidine] analogues for inhibition of histamine release. *J. Med. Chem.* 24 (2), 194−198.

(70) Sharma, P., Kumar, A., Sahu, V., Upadhyay, S., and Singh, J. (2009) Synthesis of bioactive spiro-2-[3′-(2′-phenyl)-3H-indolyl]-1-aryl-3-phenylaziridines and SAR studies on their antimicrobial behavior. *Med. Chem. Res.* 18 (5), 383−395.

(71) Saraswat, P., Jeyabalan, G., Hassan, M. Z., Rahman, M. U., and Nyola, N. K. (2016) Review of synthesis and various biological activities of spiro heterocyclic compounds comprising oxindole and pyrrolidine moities. *Synth. Commun.* 46 (20), 1643−1664.

(72) Mohan, S., Kerry, P. S., Bance, N., Niikura, M., and Pinto, B. M. (2014) Serendipitous discovery of a potent influenza virus a neuraminidase inhibitor. *Angew. Chem., Int. Ed.* 53 (4), 1076−1080.

(73) Savarino, A., Cauda, R., and Cassone, A. (2005) Aspartic proteases of Plasmodium falciparum as the target of HIV-1 protease inhibitors. *J. Infect. Dis.* 191 (8), 1381−1382.

(74) Tacconelli, E., Savarino, A., Bernardis, F. D., Cauda, R., and Cassone, A. (2004) Candidiasis and HIV-Protease Inhibitors: The Expected and the Unexpected. *Curr. Med. Chem.: Immunol., Endocr. Metab. Agents* 4 (1), 49−59.

(75) Machado, M., Sanches-Vaz, M., Cruz, J. P., Mendes, A. M., and Prudencio, M. (2017) Inhibition of Plasmodium Hepatic Infection by Antiretroviral Compounds. *Front. Cell. Infect. Microbiol.* 7, 329.

(76) Sonoiki, E., Nsanzabana, C., Legac, J., Sindhe, K. M., DeRisi, J., and Rosenthal, P. J. (2017) Altered Plasmodium falciparum Sensitivity to the Antiretroviral Protease Inhibitor Lopinavir Associated with Polymorphisms in pfmdr1. *Antimicrob. Agents Chemother.* 61 (1), e01949−16.

(77) Garcia-Sastre, A. (2017) Ten Strategies of Interferon Evasion by Viruses. *Cell Host Microbe* 22 (2), 176−184.

(78) King, T., and Lamb, T. (2015) Interferon-gamma: The Jekyll and Hyde of Malaria. *PLoS Pathog.* 11 (10), e1005118.

(79) Sullivan, A., Edlund, C., and Nord, C. E. (2001) Effect of antimicrobial agents on the ecological balance of human microflora. *Lancet Infect. Dis.* 1 (2), 101−114.

(80) DeGruttola, A. K., Low, D., Mizoguchi, A., and Mizoguchi, E. (2016) Current Understanding of Dysbiosis in Disease in Human and Animal Models. *Inflamm Bowel Dis* 22 (5), 1137−1150.

(81) *Guidance for Industry. Vaginal Microbicides: Development for the Prevention of HIV Infection*; Food and Drug Administration, Center for Drug Evaluation and Research (CDER), 2014.

(82) Hillier, S. L. (1998) The vaginal microbial ecosystem and resistance to HIV. *AIDS Res. Hum. Retroviruses* 14 (Suppl 1), S17−521.

(83) Berthold, M. R., Cebron, N., Dill, F., Gabriel, T. R., Kotter, T., Meinl, T., Ohl, P., Sieb, C., Thiel, K., and Wiswedel, B. (2008) KNIME: The Konstanz Information Miner. *Data Analysis, Machine Learning and Applications*, 319−326.

(84) Wolber, G., and Langer, T. (2005) LigandScout: 3-d pharmacophores derived from protein-bound Ligands and their use as virtual screening filters. *J. Chem. Inf. Model.* 45 (1), 160−169.

(85) Inte:Ligand *iCon, Part of LigandScout*, 4.1; Vienna, Austria 2017.

(86) MarvinSketch (version 17.22.0), Calculation module developed by ChemAxon, http://www.chemaxon.com/products/marvin/marvinsketch/, 2019.

(87) O'Boyle, N. M., Banck, M., James, C. A., Morley, C., Vandermeersch, T., and Hutchison, G. R. Open Babel: An open chemical toolbox. *J. Cheminf.* 2011, 3 (33), DOI: 10.1186/1758-2946-3-33.

(88) Steinbeck, C., Han, Y. Q., Kuhn, S., Horlacher, O., Luttmann, E., and Willighagen, E. (2003) The Chemistry Development Kit (CDK): An open-source Java library for chemo- and bioinformatics. *J. Chem. Inf Comp Sci.* 43 (2), 493−500.

(89) Toth, M. V., and Marshall, G. R. (1990) A Simple, Continuous Fluorometric Assay for Hiv Protease. *Int. J. Pept. Protein Res.* 36 (6), 544−550.

(90) Nakayama, G. R., Caton, M. C., Nova, M. P., and Parandoosh, Z. (1997) Assessment of the Alamar Blue assay for cellular growth and viability in vitro. *J. Immunol. Methods* 204 (2), 205−208.

(91) Davis, K. L., Bibollet-Ruche, F., Li, H., Decker, J. M., Kutsch, O., Morris, L., Salomon, A., Pinter, A., Hoxie, J. A., Hahn, B. H., Kwong, P. D., and Shaw, G. M. (2009) Human immunodeficiency virus type 2 (HIV-2)/HIV-1 envelope chimeras detect high titers of broadly reactive HIV-1 V3-specific antibodies in human plasma. *J. Virol.* 83 (3), 1240−1259.

(92) Reed, L. J., and Muench, H. (1938) A simple method of estimating fifty percent endpoints. *Am. J. Epidemiol.* 27, 493−497.

(93) Borrego, P., Calado, R., Marcelino, J. M., Pereira, P., Quintas, A., Barroso, H., and Taveira, N. (2013) An ancestral HIV-2/SIV peptide with potent HIV-1 and HIV-2 fusion inhibitor activity. *AIDS* 27, 1081−1090.

(94) Lara, H. H., Trevino, G. E. N., De Zamacona, M. E., Mureyko, L., and Ixtepan-Turrent, L. (2014) Luciferase Time-based, High-throughput Screening Assay for the Discovery of HIV-1Inhibitors. *J. Human Virol. Retrovirol.* 1 (3), 1−7.

(95) Ploemen, I. H., Prudencio, M., Douradinha, B. G., Ramesar, J., Fonager, J., van Gemert, G. J., Luty, A. J., Hermsen, C. C., Sauerwein, R. W., Baptista, F. G., Mota, M. M., Waters, A. P., Que, I., Lowik, C. W., Khan, S. M., Janse, C. J., and Franke-Fayard, B. M. (2009) Visualisation and quantitative analysis of the rodent malaria liver stage by real time imaging. *PLoS One* 4 (11), e7881.

(96) Mendes, A. M., Albuquerque, I. S., Machado, M., Pissarra, J., Meireles, P., and Prudencio, M. Inhibition of Plasmodium Liver Infection by Ivermectin. *Antimicrob. Agents Chemother.* 2017, 61 (2), DOI: 10.1128/AAC.02005-16.